**Molecular Cell, *Volume 32***

## Supplemental Data

# A Fence-Like Coat for the Nuclear Pore Membrane

**Erik W. Debler, Yingli Ma, Hyuk-Soo Seo, Kuo-Chiang Hsia, Thomas R. Noriega, Günter Blobel, and André Hoelz**

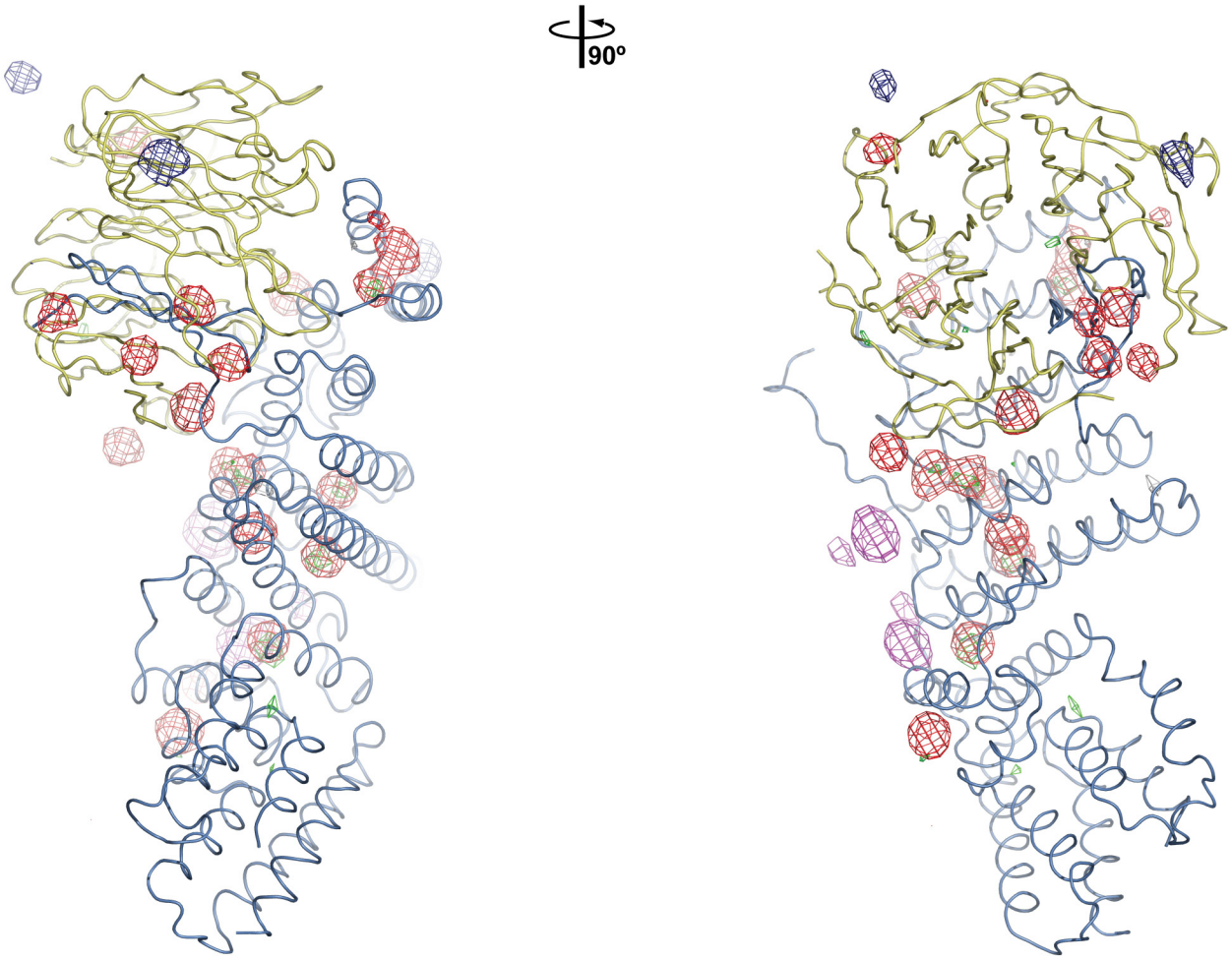


**Figure S1. Experimental Phasing.** Anomalous difference Fourier maps, illustrating selenium (red), osmium (blue), mercury (green), and $[Ta_6Br_{12}]^{2+}$ cluster (magenta) sites, calculated from x-ray diffraction data obtained from the monoclinic crystal form. A 90° rotated view is shown on the right. For clarity, only one Seh1•Nup85 heterodimer in the asymmetric unit is shown.

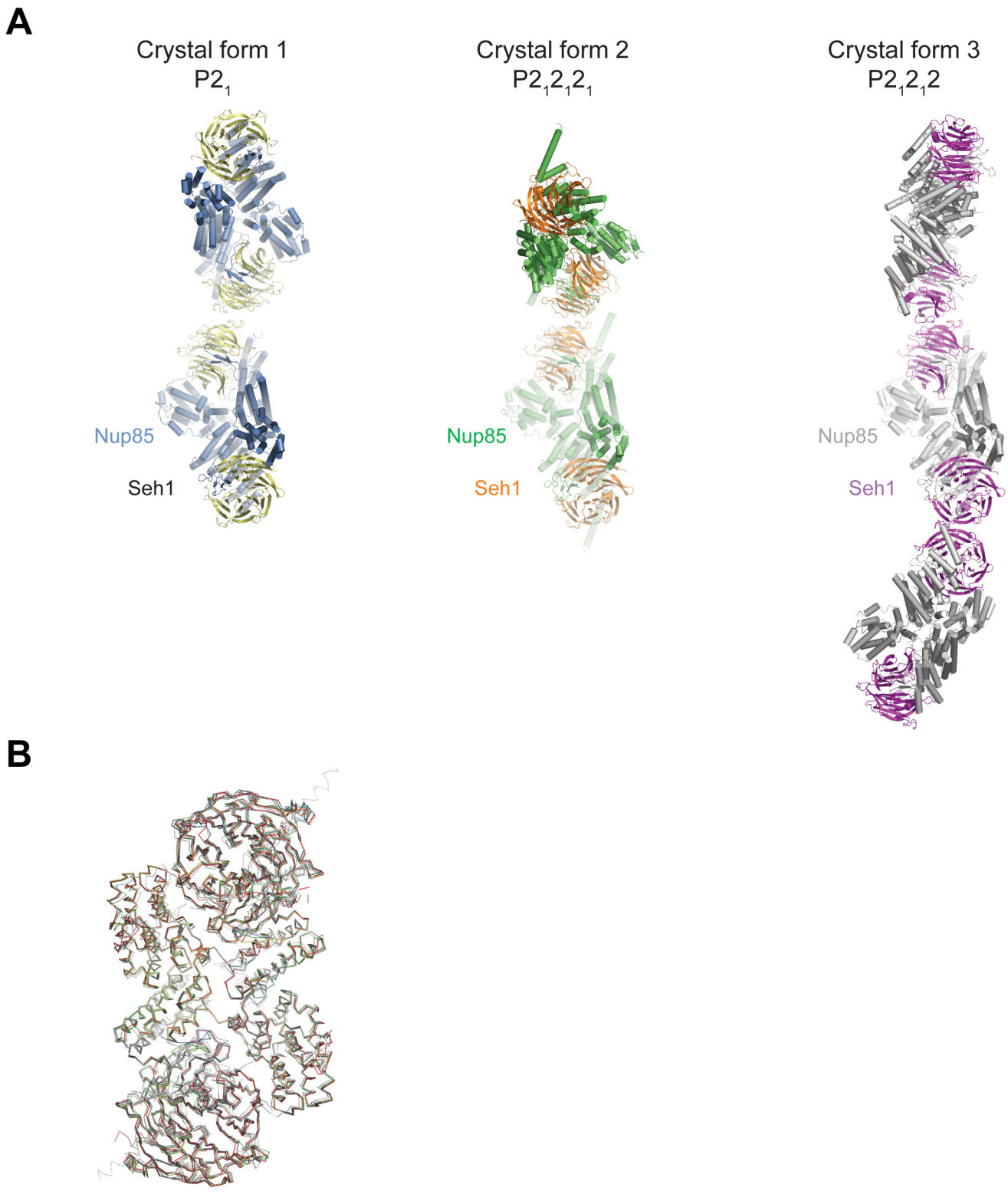


**Figure S2. Comparison of the Structures Derived from Three Different Crystal Forms.** (**A**) The asymmetric unit of crystal form 1 (left panel) and 2 (middle panel) each contained one hetero-octamer, while crystal form 3 (right panel) harbored one heterododecamer. The three structures are aligned with respect to the bottom heterotetramer of crystal form 1, and are shown in an identical orientation. The Seh1 and Nup85 molecules of the aligned heterotetramers are indicated. (**B**) Superimposition of the seven crystallographically independent Seh1•Nup85 heterotetramers of the three crystal forms, illustrating that they display little conformational plasticity and form a rigid unit.

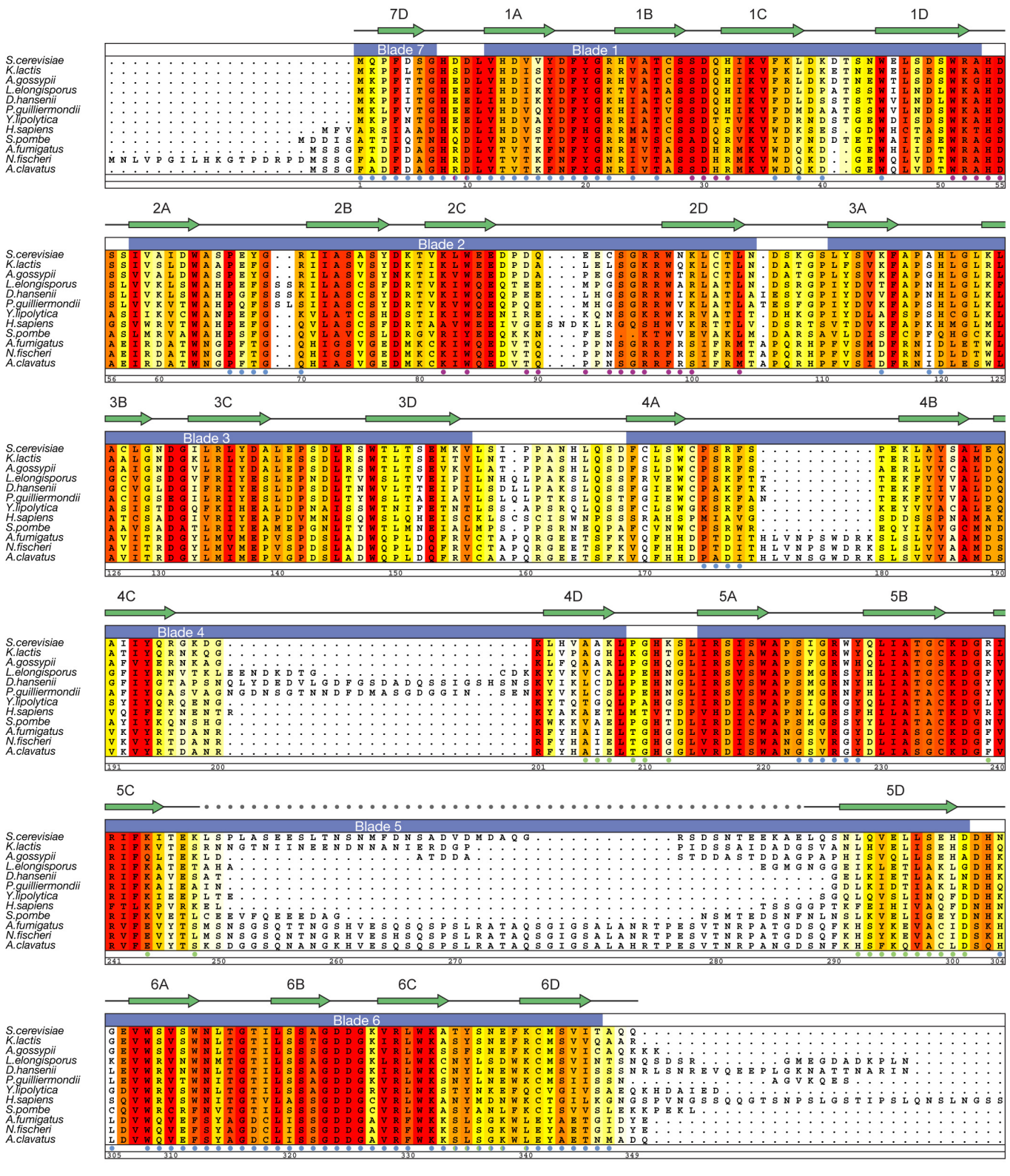


**Figure S3. Multi-Species Sequence Alignment of Seh1 Homologs.** The numbering below the alignment is relative to *S. cerevisiae* Seh1. The overall sequence conservation at each position is shaded in a color gradient from yellow (40% similarity) to dark red (100% conservation) using the Blosum62 weighting algorithm. The secondary structure is indicated above the sequence as green arrows (β-strands), gray lines (coil regions), and gray dots (disordered residues). The participation of various residues in the formation of the Seh1•Seh1 dimerization interface (purple dots), the Seh1•Nup85 interface within the heterodimer (blue dots), and the Seh1•Nup85 interface with an adjacent Seh1•Nup85 heterodimer (green dots) is indicated below the aligned sequences.

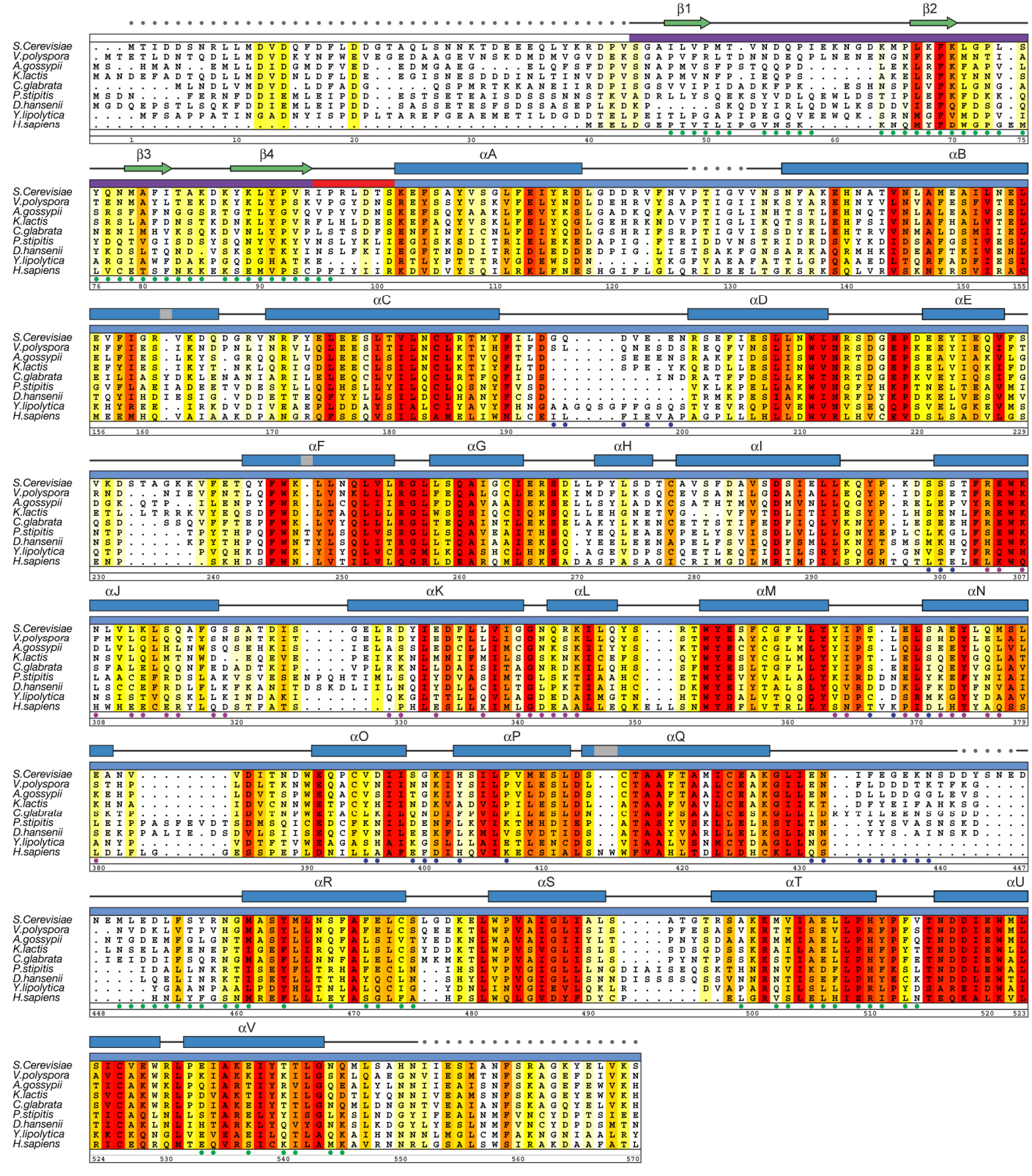


**Figure S4. Multi-Species Sequence Alignment of Nup85 Homologs.** The alignment is generated and colored according to Figure S3. The secondary structure is indicated above the sequence as green arrows (β-strands), blue rectangles (α-helices), gray lines (coil regions), and gray dots (disordered residues). The numbering below the alignment is relative to *S. cerevisiae* Nup85. The participation of various residues in the interface between Seh1 and Nup85 within the Seh1•Nup85 heterodimer (green dots), and the interface between two Seh1•Nup85 heterodimers (purple dots, Seh1 interaction; blue dots, Nup85 interaction) is indicated below the aligned sequences.

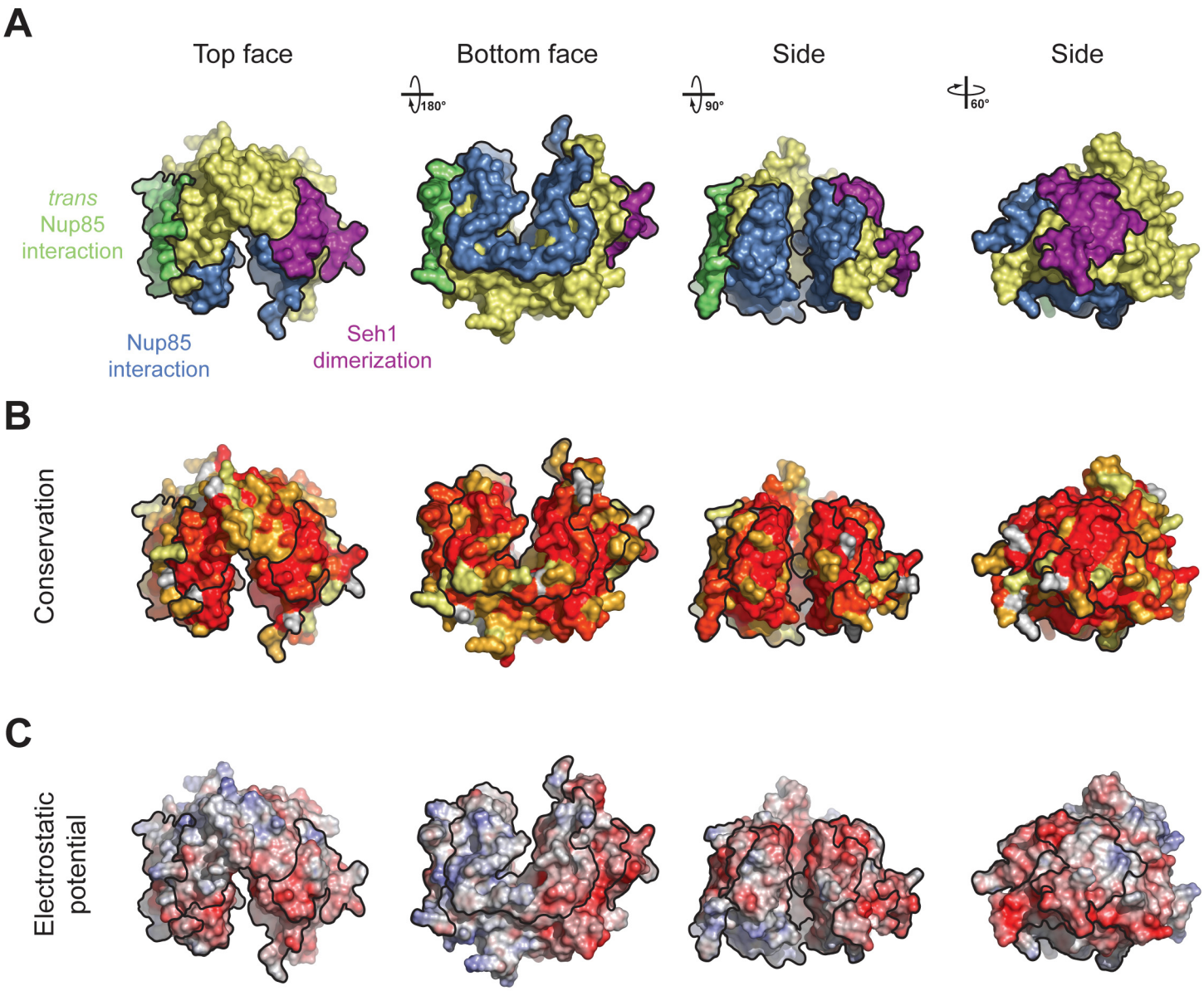


**Figure S5. Surface Properties of Seh1.** (**A**) Surface rendition of Seh1 (yellow), illustrating the participation of various surface patches in the interaction with Nup85 (within the heterodimer, blue; with an adjacent heterodimer, green) and the homodimerization with an adjacent Seh1 (purple). (**B**) Surface rendition of Seh1, colored according to sequence conservation from 40 % similarity (yellow) to 100 % conservation (red). (**C**) Surface rendition of Seh1, colored according to the electrostatic potential, ranging from red (-15 $k_B$T/e) to blue (+15 $k_B$T/e). The various interface borders are indicated by black lines.

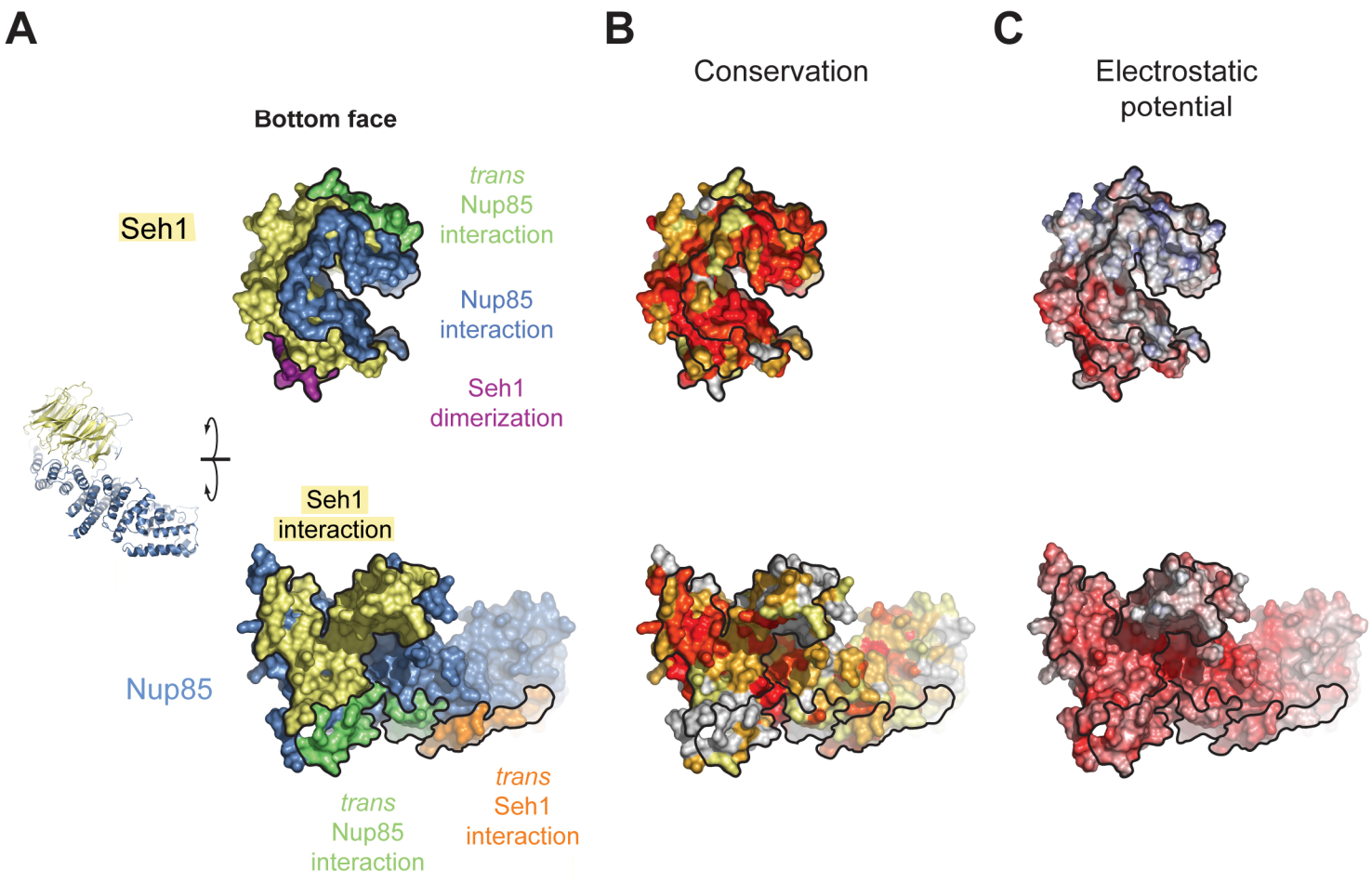


**Figure S6. Surface Properties of the Seh1•Nup85 Interaction.** (**A**) Surface renditions of Nup85 and Seh1 in an open book representation. The Seh1 surface is colored according to Figure S5. The Nup85 surface (blue) is colored according to the participation of various surface patches in the interaction with Seh1 within the heterodimer (yellow), with Seh1 of the adjacent heterodimer (orange), and with the adjacent Nup85 (green). (**B**) Nup85 is colored according to sequence conservation, from 40 % similarity (yellow) to 100 % conservation (red). (**C**) Surface rendition of Nup85, colored according to the electrostatic potential, ranging from red (-15 $k_BT/e$) to blue (+15 $k_BT/e$). The various interface borders are indicated by black lines.

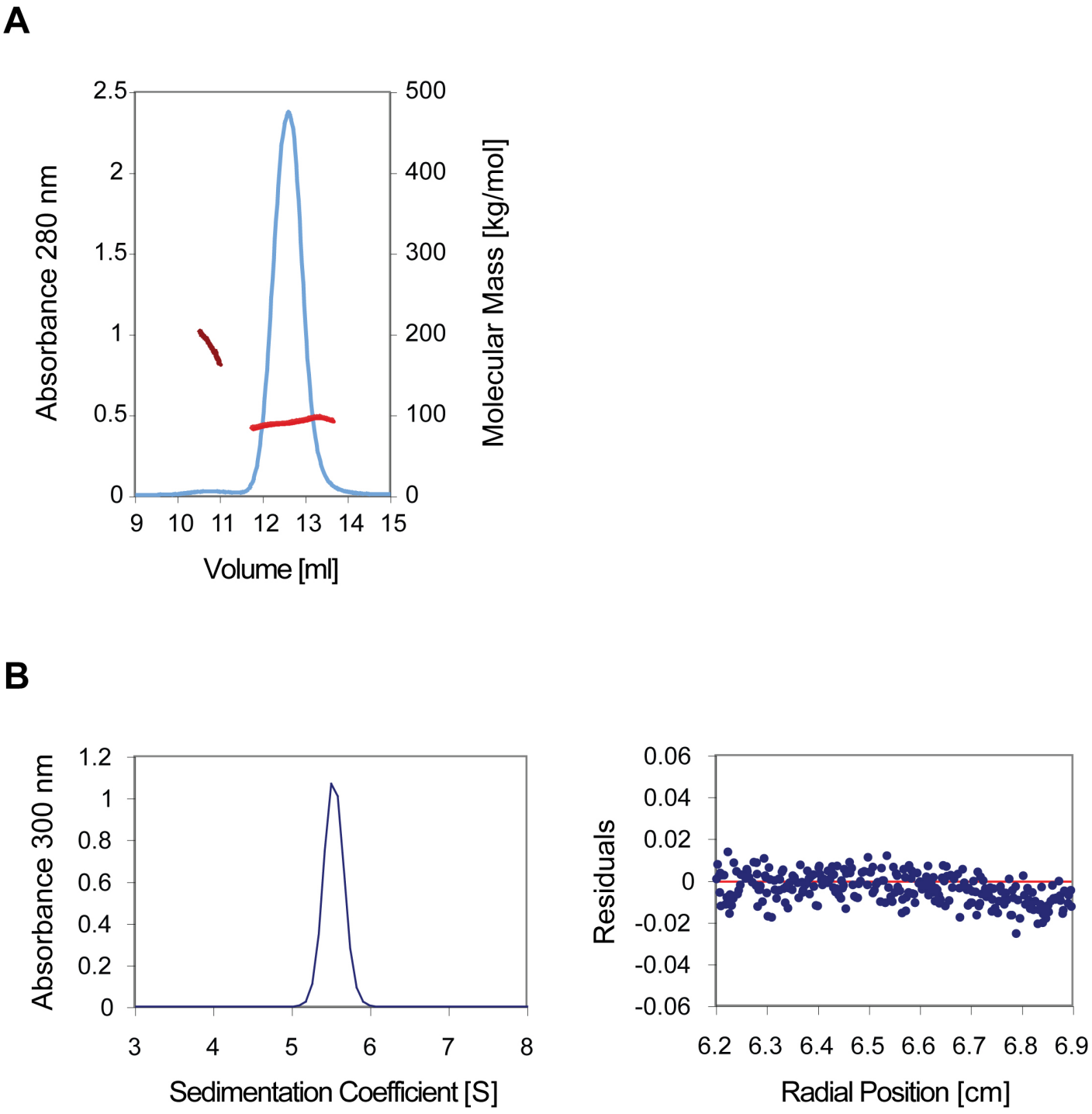


**Figure S7. Oligomerization of Seh1•Nup85 in Solution. (A)** Gel filtration profile of Seh1•Nup85 on Superdex 200 HR 10/300 (GE Healthcare) coupled to multi-angle light scattering (MALS) analysis. The molecular weights of the minor and major peak (heterodimer and heterotetramer, respectively) as determined by MALS are indicated. **(B)** Sedimentation velocity analysis of Seh1•Nup85. The sedimentation coefficient distribution c(s) (left panel) shows a single species that corresponds to the Seh1•Nup85 heterodimer. The residuals for the single exponential fit are shown in the right panel.

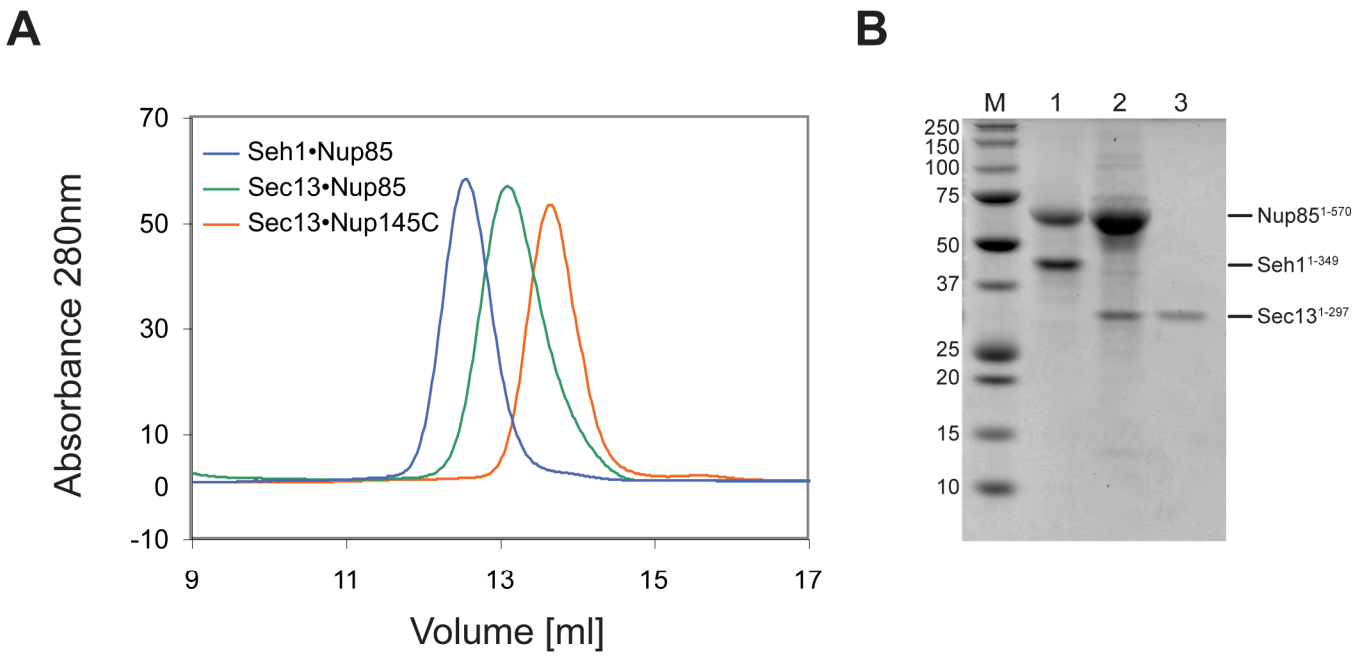


**Figure S8. Biochemical Analysis of the Sec13•Nup85 Complex.** (**A**) Sec13 can form a stable complex with Nup85 when co-expressed in *E.coli*. Gel filtration profiles of the Seh1•Nup85 complex (blue), the Sec13•Nup85 complex (green), and the Sec13•Nup145C complex (red) are shown. The complexes were co-purified to homogeneity and the peak fractions of the final gel filtration step were analyzed by SDS-PAGE and Coomassie-staining. (**B**) Coomassie-stained SDS-PAGE gel illustrating the peak fractions of the Seh1•Nup85 complex (lane 1), of the Sec13•Nup85 complex (lane 2) and as a reference Sec13 (lane 3). The identity of the various proteins has been confirmed by N-terminal sequencing and mass spectrometry.

## Table S1. Crystallographic Analysis of Crystal Form 2

| | Crystal 1<br>Native | Crystal 2<br>$K_2OsO_4$ | Crystal 3<br>$[Ta_6Br_{12}]^{2+}$ |
|---|---|---|---|
| **Data collection** | | | |
| Synchrotron | APS[a] | APS[a] | APS[a] |
| Beamline | GM/CA-CAT 23ID-D | NE-CAT 24ID-C | NE-CAT 24ID-C |
| Space group | $P2_12_12_1$ | $P2_12_12_1$ | $P2_12_12_1$ |
| Cell dimensions | | | |
| *a*, *b*, *c* (Å) | a=105.4, b=106.5, | a=110.5, b=110.7, | a=112.1, b=112.2, |
| | c=358.6 | c=364.1 | c=354.0 |
| $\alpha, \beta, \gamma$ (°) | $\alpha=\beta=\gamma=90$ | $\alpha=\beta=\gamma=90$ | $\alpha=\beta=\gamma=90$ |
| | | *Os Peak* | *Ta Peak* |
| Wavelength (Å) | 1.03319 | 1.1399 | 1.2546 |
| Resolution (Å) | 50.0-3.75 | 50.0-5.2 | 50.0-7.3 |
| $R_{sym}$ (%)[b] | 18.0 (75.3) | 11.8 (59.7) | 13.7 (73.6) |
| $\langle I / \sigma I \rangle$ [b] | 7.8 (1.9) | 11.3 (1.7) | 11.1 (2.2) |
| Completeness (%)[b] | 96.2 (94.8) | 96.2 (86.1) | 100.0 (100.0) |
| Redundancy[b] | 5.4 (4.6) | 5.5 (2.7) | 5.6 (5.6) |
| **Refinement** | | | |
| Resolution (Å) | 50.0 – 3.75 | | |
| No. reflections | 39,143 | | |
| Test set | 1,972 (4.7 %) | | |
| $R_{work}$ / $R_{free}$ (%) | 24.3 / 27.2 | | |
| No. atoms | 25,114 | | |
| R.m.s deviations | | | |
| Bond lengths (Å) | 0.010 | | |
| Bond angles (°) | 1.4 | | |
| Ramachandran plot[c] | | | |
| Most favored (%) | 78.6 | | |
| Additionally allowed (%) | 20.5 | | |
| Generously allowed (%) | 0.8 | | |
| Disallowed (%) | 0.1 | | |

[a]APS, Advanced Photon Source, Argonne National Laboratory

[b]Highest-resolution shell is shown in parentheses.

[c]As determined by Procheck.

## Table S2. Crystallographic Analysis of Crystal Form 3

| | Crystal 1<br>SeMet | Crystal 2<br>SeMet |
|---|---|---|
| **Data collection** | | |
| Synchrotron | APS[a] | APS[a] |
| Beamline | GM/CA-CAT 23ID-B | GM/CA-CAT 23ID-B |
| Space group | $P2_12_12$ | $P2_12_12$ |
| Cell dimensions | | |
| *a*, *b*, *c* (Å) | a=210.2, | a=210.7, |
| | b=226.5, | b=227.9, |
| | c=190.6 | c=191.6 |
| $\alpha, \beta, \gamma$ (°) | $\alpha=\beta=\gamma=90$ | $\alpha=\beta=\gamma=90$ |
| | | *Se Peak* |
| Wavelength (Å) | 1.0332 | 0.9795 |
| Resolution (Å) | 50.0-3.2 | 50.0-3.35 |
| $R_{sym}$ (%)[b] | 14.5 (72.9) | 17.9 (54.1) |
| $\langle I / \sigma I \rangle$ [b] | 10.7 (2.0) | 6.9 (2.2) |
| Completeness (%)[b] | 99.2 (97.9) | 98.3 (93.4) |
| Redundancy[b] | 4.9 (4.3) | 3.7 (3.5) |
| | | |
| **Refinement** | | |
| Resolution (Å) | 50.0-3.2 | |
| No. reflections | 129,823 | |
| Test set | 6,534 (4.4 %) | |
| $R_{work}$ / $R_{free}$ (%) | 26.1 / 28.1 | |
| No. atoms | 37,807 | |
| R.m.s deviations | | |
| Bond lengths (Å) | 0.008 | |
| Bond angles (°) | 1.4 | |
| Ramachandran plot[c] | | |
| Most favored (%) | 83.8 | |
| Additionally allowed (%) | 15.6 | |
| Generously allowed (%) | 0.5 | |
| Disallowed (%) | 0.1 | |

[a]APS, Advanced Photon Source, Argonne National Laboratory

[b]Highest-resolution shell is shown in parentheses.

[c]As determined by Procheck.